HHS Public Access

Author manuscript

Cell Rep. Author manuscript; available in PMC 2016 August 11.

Published in final edited form as:

Cell Rep. 2015 August 11; 12(6): 903–912. doi:10.1016/j.celrep.2015.07.020.

Hox5 genes regulate the *Wnt2/2b-Bmp4* signaling axis during lung development

Steven M. Hrycaj[1], **Briana R. Dye**[2], **Nicholas C. Baker**[1], **Brian M. Larsen**[1], **Ann C. Burke**[3], **Jason R. Spence**[2], and **Deneen M. Wellik**[1,2,*]

[1]Department of Internal Medicine, Division of Molecular Medicine and Genetics, University of Michigan, Ann Arbor, MI 48109-2200, USA

[2]Department of Cell and Developmental Biology, University of Michigan, Ann Arbor, MI 48109-2200, USA

[3]Department of Biology, Wesleyan University, Middletown, CT 06459, USA

Abstract

Hox genes are required for proper anteroposterior axial patterning and the development of several organ systems. Herein, we show that all three *Hox5* paralogous genes play redundant roles in the developing lung. *Hoxa5;Hoxb5;Hoxc5* triple mutant embryos develop severely hypoplastic lungs with reduced branching and proximal-distal patterning defects. *Hox5* genes are exclusively expressed in the lung mesoderm, however, defects are observed in both lung mesenchyme and endodermally-derived epithelium, demonstrating that *Hox5* genes act to regulate mesodermal-epithelial crosstalk during development. We show that *Hox5* loss-of-function leads to loss of *Wnt2/2b* expression in the distal lung mesenchyme and the down-regulation of previously identified downstream targets of *Wnt2/2b* signaling including *Lef1*, *Axin2* and *Bmp4*. Wnt2/2b-enriched media rescues proper Sox2/Sox9 patterning and restores *Bmp4* expression in *Hox5* triple mutant lung explants. Taken together, these data show that *Hox5* genes are key upstream mesenchymal regulators of the *Wnt2/2b-Bmp4* signaling axis critical for proper lung patterning.

Graphical Abstract

*Corresponding Author: Deneen M. Wellik, PhD, dwellik@umich.edu, University of Michigan Medical Center, 109 Zina Pitcher, 2053 BSRB, Ann Arbor, MI 48109-2200, Phone: 734-936-8902, FAX: 734-763-2162.

Author Contributions:

S.M.H. co-developed the concept, performed experiments, analyzed data and co-wrote the manuscript. B.R.D., N.C.B., and B.M.L. performed experiments. A.C.B. contributed reagents. J.R.S. contributed reagents and advice. D.M.W. developed the concept, co-wrote the manuscript and supervised the project. All authors reviewed drafts of the manuscript.

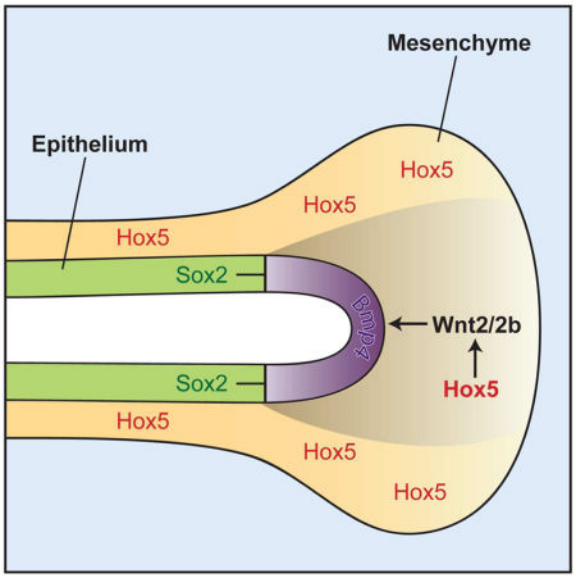

Introduction

Lung specification begins around embryonic day E9.0 in the mouse with expression of the transcription factor *Nkx2.1* in the ventral anterior foregut endoderm (Herriges and Morrisey, 2014; Morrisey and Hogan, 2010). By E9.5, two primary lung buds have emerged from the endoderm, surrounded by associated mesoderm. The two lung buds undergo a stereotyped process of branching morphogenesis that results in the generation of a complex arborized network of gas-delivering bronchioles and gas-exchanging alveoli. Concomitant with lung branching, a complex network of signaling pathways and transcription factors governs the process of lung bud growth and patterning. Early lung epithelium is initially patterned into proximal airway progenitors that express Sox2 and distal airway progenitors that express Sox9 (Chang et al., 2013; Rockich et al., 2013; Tompkins et al., 2011). The proximal-distal (PD) pattern of the lung is established in part by the Wnt/β-catenin, Bmp and Fgf signaling networks (Mucenski et al., 2003; Weaver et al., 1999; Yin et al., 2008). How these networks are established and are related to one another at a mechanistic level is complex.

Hox genes are a deeply conserved group of transcription factors that provide important patterning cues along the AP axis of the vertebral skeleton and the PD axis of the limb skeleton (Mallo et al., 2010). A multitude of additional roles for this group of genes have also been reported that encompass many aspects of organogenesis (Di Meglio et al., 2013; Manley and Capecchi, 1998; Rousso et al., 2008; Wellik et al., 2002; Xu et al., 2013; Yallowitz et al., 2011). In mammals, 39 *Hox* genes are arranged collinearly in four clusters and can be categorized into thirteen paralogous groups based on sequence similarity and position within the cluster (Kessel and Gruss, 1990). A high degree of sequence similarity and functional redundancy exists among paralogous groups (Mallo et al., 2010). As a result, genetic loss of function of a single gene within a paralogous group often results in no or incompletely penetrant phenotypes whereas mutants for the entire paralogous group exhibit extensive defects.

Previous studies have shown that single *Hoxa5* mutant and compound *Hoxa5;b5* double mutant mice have abnormal growth and branching of the lungs during embryonic development that results in semi-penetrant neonatal lethality (Aubin et al., 1997; Boucherat et al., 2013). To explore the possibility that retention of the remaining paralog, *Hoxc5*, is masking redundant functions in the lung, we generated *Hoxa5;Hoxb5;Hoxc5* triple mutant animals. *Hox5* triple mutants display dramatically more severe phenotypes than single or double mutants, demonstrating functional redundancy among *Hox5* genes during lung development. In *Hox5* triple mutants, lung specification and budding is unaffected but severe growth and patterning defects are observed. Complete loss of *Hox5* function leads to loss of Wnt/β-catenin signaling in the distal lung mesenchyme accompanied by corresponding down-regulation of several previously identified downstream targets of canonical Wnt/β-catenin signaling including mesenchymal *Lef1* expression, and *Axin2* and *Bmp4* expression in the distal epithelium (Yin et al., 2008). *Hox5* triple mutant lungs also exhibit PD-patterning defects as evidenced by the distal expansion of mesenchymal Sox9 and epithelial Sox2 expression. Finally, we show that *Hox5* triple mutant lung explants cultured in Wnt2/2b-enriched media rescues the branching phenotype, restores proper Sox2/Sox9 PD patterning and normalizes *Bmp4* expression in the distal epithelium. Thus, these data demonstrate that *Hox5* is a critical upstream regulator of *Wnt2/2b* in the distal lung mesenchyme and identify a *Hox5-Wnt2/2b-Bmp4* signaling axis from the mesenchyme to the epithelium that is critical for the proper growth and PD patterning of the lung during embryogenesis.

Results

Complete loss of Hox5 function leads to dramatic lung defects

Generation of *Hox5* mutant animals resulted in data that is consistent with previous work that reported the abnormal growth and branching phenotype of the lungs from single *Hoxa5* mutant (*Hox5 aaBBCC*) mice are exacerbated in *Hoxa5;Hoxb5* double mutants (*Hox5 aabbCC*) compared to controls at E18.5 (Figure 1A) (Aubin et al., 1997; Boucherat et al., 2013). In contrast, *Hoxb5* and *Hoxc5* single mutants and *Hoxb5;Hoxc5* double mutants (*Hox5 AAbbcc*) are viable with no obvious defects in lung development, consistent with a previous report suggesting *Hoxc5* may not function in the development of this organ (Boucherat et al., 2013). However, when examined genetically, removal of *Hoxc5* function in addition to *Hoxa5* and *Hoxb5* (*Hox5 aabbcc* triple mutants) results in an extreme exacerbation of lung defects (Figure 1A). Lungs from *Hox5* triple mutant animals are severely hypoplastic and have dramatic growth and patterning defects.

Hox5 genes are exclusively expressed in the mesoderm of the embryonic lung

qPCR analyses of *Hoxa5*, *Hoxb5* and *Hoxc5* expression levels in the developing lung reveal that the expression levels of all three *Hox5* paralogs are highest at early stages of lung development (Figure 1B). During subsequent embryonic stages, the expression levels of *Hoxb5* and *Hoxc5* decrease. In contrast, *Hoxa5* maintains a relatively high level of expression through E18.5. *In situ* hybridization (*ISH*) analyses using combined probes for all three *Hox5* genes show that *Hox5* genes are exclusively expressed in the lung mesenchyme and not expressed in the epithelium at any embryonic stage examined (Figure 1C). At E11.5,

Hox5 shows the strongest expression in the distal mesenchyme and appears more uniformly expressed throughout the mesenchyme at E12.5 and E14.5.

Hox5 triple mutant lungs exhibit PD patterning defects

Previous studies have shown that the expression of two transcription factors, *Sox2* and *Sox9*, serve as early molecular markers of proximal and distal airway in the developing lung (Chang et al., 2013; Rockich et al., 2013; Tompkins et al., 2011). In wild-type lungs, Sox9 is exclusively expressed in the mesoderm (and not epithelium) in the proximal airway and only in the epithelium (and not mesoderm) in the distal airway, while Sox2 is exclusively expressed in the proximal airway epithelium. As depicted in Figure 1D, this stereotypical PD patterning is disrupted in *Hox5* triple mutant lungs with mesenchymal Sox9 expression extending into distal regions of the airway and epithelial expression of Sox9 only detected in the outer most edges of the *Hox5* mutant lung at E14.5 compared to controls. Consistent with these data, whole mount IHC analyses of Sox2/Sox9 expression in E14.5 lungs show a clear expansion of mesenchymal Sox9 expression into more distal regions of the lung in *Hox5* triple mutants (Figure S1A, arrowheads). Despite this, the expanded mesenchymal Sox9 expression does not lead to the formation of ectopic cartilage in this region (Figure S1B).

Loss of Hox5 function disrupts the normal differentiation of distal lung epithelial cell types

Figure 1A demonstrates that *Hox5* triple mutant lungs exhibit severe defects in lung development by E18.5. H&E staining of histological sections at E18.5 shows that *Hox5* triple mutant lungs have fewer saccules and an overall thickening of the lung parenchyma in the distal airway (Figure 1E). Normally, two types of cells populate the distal epithelium at newborn stages; squamous AECI cells that allow gas exchange and cuboidal AECII cells that produce surfactant. Anti-E-cadherin staining reveals an increase in the number of cuboidal epithelial cells in the distal airway in mutants compared to controls (Figure 1E). Further investigation of the distribution of AECI and AECII epithelial cells demonstrates significant perturbations in these populations in *Hox5* triple mutants. Immunostaining for Aqp5, which specifically marks AECI cells, shows large stretches of lung epithelium that are devoid of Aqp5 expression in the distal lungs of *Hox5* triple mutants (Figure 1E). This is never observed in controls. Analysis of the AECII-specific proteins Sftpc and SP-B in control and *Hox5* triple mutant lungs reveal an increase in the number of AECII cells in the distal airway of mutants at E18.5 (Figure 1E). Further investigation using antibodies against cell types specific to the proximal airway and trachea (secretory, ciliated, basal and PNEC cells) reveal distal regions are negative for all proximal markers examined and that overall distribution of these cell types are unaffected in *Hox5* triple mutants (Figure S1C). Thus, these data suggest that the *Hox5* genes play a critical role in the specification of AECI cells during lung development.

Lung initiation events are unaffected in Hox5 triple mutants

Lung bud initiation events are morphologically indistinguishable between controls and *Hox5* triple mutants (Figure 2A). In addition, the expression patterns of factors previously shown to be important for lung initiation events including Nkx2.1, *Raldh2* and *Shh* are unaffected

in *Hox5* triple mutants compared to controls (Figure 2B) (Bellusci et al., 1997; Kimura et al., 1996; Mollard et al., 2000). In contrast, by E12.5, *Hox5* triple mutant lungs are visibly hypoplastic and exhibit a statistically significant reduction in the number of distal branch tips compared to controls (Controls = 19.66 ± 1.53 compared to *Hox5* triple mutants = 11.33 ± 0.58 distal branch tips) (Figure 2A). By E14.5, the *Hox5* triple mutant lung phenotype is more severe with a greater relative reduction in size and more pronounced branching defects (Figure 2A). Quantification reveals that *Hox5* triple mutants exhibit an overall reduction of ≈85% of total lung volume of the left lobe and ≈65% of the right lobes compared to controls (Figure S2A). Despite this observation, we measure no difference in the expression levels of any of the three *Hox5* genes by qPCR, and ISH analyses show uniform expression of *Hox5* in both the right and left lobes at E12.5 (Figure S2B). Furthermore, there are no measureable differences in cell proliferation in either the lung epithelium or mesenchyme of *Hox5* triple mutants at E14.5 (Figure S2A).

Fgf and Shh pathways are unaffected in Hox5 triple mutant lungs

Several conserved signaling pathways are critical for proper lung development (Herriges and Morrisey, 2014; Morrisey and Hogan, 2010). Fgf9, Fgf10 and Shh signaling are critical in directing the proper growth and branching of the lung epithelium during early lung morphogenesis (Bellusci et al., 1997; Sekine et al., 1999; Yin et al., 2008). qPCR analyses show no statistical difference in the expression levels of *Fgf9*, *Fgf10*, *Spry2*, *Gli1* or *Ptch1* in *Hox5* triple mutants compared to controls at both E12.5 or later in development, at E14.5 (Figures 2C; S2C). Consistent with these data, ISH analyses of *Etv5*, a downstream target of *Fgf* signaling expressed in the distal epithelium, and *Shh* expression in the lung epithelium show no change in their expression patterns in *Hox5* triple mutants at both E12.5 or E14.5 (Figures 2C; S2D). Consistent with the lack of defects in Fgf signaling, E12.5 control and mutant epithelia respond equivalently in the presence of Fgf10 (Figure S3A).

Hox5 genes regulate canonical Wnt/β-catenin signaling

It has been previously reported that both *Wnt2* and *Wnt2b*, ligands of the canonical Wnt/β-catenin signaling pathway, are exclusively expressed in the lung mesoderm in the distal lung during early embryonic stages (Miller et al., 2012). Similar to *Wnt2/2b*, *Hox5* is also expressed in the lung mesenchyme. In order to evaluate a potential relationship, we first performed *Wnt2* and *Hox5* ISH analyses on adjacent sections at E11.5. These results demonstrate that *Hox5* and *Wnt2* are expressed in a nearly identical pattern in the distal mesenchyme at this stage (Figure 3A). Moreover, ISH for a Wnt/β-catenin target, *Lef1*, on an adjacent section, reveals that *Lef1* expression also overlaps with both *Hox5* and *Wnt2* in the distal mesenchyme (Figure 3A). To determine if Wnt signaling is perturbed in *Hox5* mutants, we performed qPCR analyses for several components of the Wnt/β-catenin signaling pathway. These analyses revealed a significant reduction of the expression levels of both *Wnt2* and *Wnt2b* in *Hox5* triple mutant lungs compared to controls while the expression levels of other Wnt pathway components remain unchanged at E14.5 (Figure 3A). Of note, the expression levels of *Wnt7a/7b*, two ligands specifically expressed in the epithelium of the distal lung are unchanged in *Hox5* triple mutants (Figure 3A). qPCR analyses also revealed that several Wnt/β-catenin target genes including *Lef1*, *Axin2*, *Bmp4*, *SMA* and *SM22*, are downregulated in *Hox5* triple mutant lungs compared to controls

(Figure 3B). Consistent with qPCR data, ISH analysis of *Wnt2* shows a dramatic reduction of signal in the distal mesenchyme of *Hox5* triple mutant lungs at E14.5 while expression levels of *Wnt7b* in the lung epithelium appear unchanged (Figure 3A). qPCR analyses at earlier developmental times (E12.5) show that *Wnt2/2b* expression is already decreased by this earlier stage and *Wnt7a/7b* levels are unchanged, similar to what is observed at E14.5 (Figure S2C).

Wnt/β-catenin signaling in the early lung mesenchyme has been shown to play an important role in airway smooth muscle progenitor expansion (Cohen et al., 2009). Because we see a dramatic reduction in the expression levels of *Wnt2/2b* and of Wnt/β-catenin target genes in the lung mesenchyme of *Hox5* triple mutants, we examined the expression of smooth muscle markers in *Hox5* triple mutant lungs by IHC and qPCR. Immunostaining for SMA expression shows a decrease, and in some cases absence, of smooth muscle development in *Hox5* triple mutant lungs (Figure 3B). Consistent with these data, qPCR analyses in *Hox5* triple mutants indicate that the expression levels of SMA and SM22 are significantly reduced compared to controls (Figure 3B).

Previous reports have shown that Wnt/β-catenin signaling is a critical upstream regulator of PD patterning in the lung, in part, through regulation of *Bmp4* signaling (Shu et al., 2005). Due to the dramatic reduction in the expression of *Wnt2/2b* in *Hox5* triple mutants (Figures 3A; S2C), we examined the expression levels of *Lef1*, *Axin2* and *Bmp4* in *Hox5* triple mutant lungs. Consistent with qPCR results, *Lef1* expression is nearly absent in the distal mesenchyme in *Hox5* triple mutant lungs, whereas expression in controls in this region is robust (Figure 3B). Next, we crossed a previously described Axin2-LacZ reporter allele (Lustig et al., 2002) into our *Hox5* mutant colony in order to examine potential changes in Axin2 expression in *Hox5* triple mutants. As depicted in Figure 3B, Axin2 is expressed in both the mesenchyme and epithelium in the distal lung at E14.5. In contrast, while Axin2 expression appears relatively unchanged in the mesenchyme, signal is absent from the epithelium in Axin2-LacZ/+;*Hox5* triple mutant lungs at E14.5. Consistent with the reporter data, additional *Axin2* ISH experiments performed at E14.5 confirm the absence of *Axin2* expression in the distal epithelium of *Hox5* triple mutant lungs throughout the lung (Figures 3B; S2E). qPCR supports the observed decrease of *Lef1* and *Axin2* signal in *Hox5* triple mutants at both E12.5 and E14.5 (Figures 3B, S2C). Finally, ISH analyses showed a dramatic down-regulation of *Bmp4* expression in the lungs of *Hox5* triple mutants compared to controls at E14.5 (Figure 3B). These changes are confirmed by qPCR (Figure 3B).

Wnt-enriched media rescues proper Sox9/Sox2 patterning and restores Bmp4 expression in the distal epithelium of Hox5 mutant lungs

Utilizing a lung explant culture system, we next tested whether the addition of Wnt2/2b is sufficient to rescue *Hox5* mutant phenotypes. Briefly, lungs of both control and *Hox5* triple mutant embryos were dissected at E12.5, cultured for 96 hours in either control or Wnt2/2b-enriched media, collected and analyzed. At the initiation of the culture conditions, *Hox5* triple mutant lung explants already demonstrated a decrease in distal branch tips (Figure 4A). By 96 hours in culture, *Hox5* mutant lung explants exhibited a ~50% decrease in the total number of distal branch tips compared to controls (controls = 84.66 ± 4.72 distal

branch tips; *Hox5* triple mutants = 41.66 ± 0.57) (Figure 4A). The addition of Wnt2/2b ligand into the culture media increased the total number of distal branch tips of *Hox5* triple mutant lungs by ~80% after 96 hours (*Hox5* triple mutants in control media = 41.66 ± 0.57; *Hox5* triple mutants in Wnt2/2b- enriched media = 74.66 ± 1.52), to nearly the same total number of distal branch tips as control lung explants (controls = 84.66 ± 4.72 distal branch tips; *Hox5* triple mutants + Wnt2/2b = 74.66 ± 1.52). These data demonstrate that the addition of Wnt2/2b ligand into the culture media almost completely normalizes the lung branch tip number in *Hox5* triple mutant lungs.

Remarkably, in addition to rescue of branch number, assessment of Sox2, Sox9 and *Bmp4* expression reveals a re-establishment of normal lung PD pattern in *Hox5* triple mutants when cultured in Wnt2/2b-enriched media (Figure 4B). Control lung explants cultured for 96 hours in control media have normally patterned airway with clear Sox2+ proximal and Sox9+ distal domains, in addition to strong *Bmp4* staining in the distal epithelium, similar to what is observed *in vivo*. In contrast, *Hox5* triple mutant explants exhibit the abnormal PD patterning observed *in vivo* with expansion of Sox2+ proximal progenitors into more distal regions of the airway, a reduction of Sox9+ distal airway progenitors, as well as reduction of the number of *Bmp4*+ branch tips compared to controls. Proper PD patterning is restored in *Hox5* mutant lung explants cultured in Wnt2/2b-enriched media for 96 hours as evidenced by the normalization of the expression domains of Sox2 and Sox9, as well as an increase in the number of *Bmp4*+ distal branch tips similar to controls. Consistent with these data, SMA immunostaining in *Hox5* triple mutant explants cultured in control media show a marked decrease, and in some areas absence, of smooth muscle development, similar to what is observed *in vivo* (Figure S3B). Culturing *Hox5* triple mutant explants in Wnt2/2b enriched media for 96 hours restores proper smooth muscle development as evidenced by the normalization of SMA expression (Figure S3B). Collectively, these data provide strong evidence that the addition of Wnt2/2b is sufficient to rescue the downstream defects in *Hox5* triple mutant lungs and is primarily responsible for the defects in *Hox5* mutant lungs.

Discussion

Hox genes have been shown to play important roles in many aspects of organogenesis, but it has been difficult to place these highly conserved transcription factors into established regulatory networks controlling development. It has been previously shown that single *Hoxa5* mutant and compound *Hoxa5;Hoxb5* double mutant mice have abnormal growth and branching of the lungs during embryonic development (Aubin et al., 1997; Boucherat et al., 2013), but the defects in these lungs are relatively mild and downstream pathways associated with these defects have not been elucidated. Due to the fact that numerous reports demonstrate functional redundancy among *Hox* paralogs, we additionally removed *Hoxc5* function to assess redundant roles that might allow the identification of pathways regulated by *Hox5* genes during lung development. Phenotypes of *Hox5* triple mutants are much more severe than previously reported for single or double mutants, indicating that *Hoxc5* plays a redundant role with its paralogs *Hoxa5* and *Hoxb5* during lung development.

Loss of all three *Hox5* paralogs results in specific defects in early lung development. Lung specification and budding proceeds normally and many early growth factors such as Shh,

Fgf9 and Fgf10 as well as RA signaling are not affected. Our data show that loss of *Hox5* function leads to dramatic down-regulation of *Wnt2* and *Wnt2b*, two critical growth factors that are also expressed in early lung mesenchyme and are required for appropriate PD patterning as well as distal expansion of the developing lung. Loss of *Wnt* signaling in the lung mesenchyme leads to the loss of canonical Wnt/β-catenin activity in the distal epithelium demonstrated by specific loss of *Axin2* staining in the distal lung epithelium, supporting a key role for *Hox5*-regulated, mesenchymal *Wnt* signaling in establishing the mesenchymal-epithelial crosstalk during early lung growth and patterning. Our data are also consistent with previous work examining targeted deletion of β-catenin in the distal lung epithelium which resulted in proximalization of the lung (Mucenski et al., 2003; Shu et al., 2005). Despite the well-established role for Wnt/β-catenin signaling in lung branching and patterning events, very little is known about the regulation of this pathway during lung development. It has been reported that FGF9 produced in the lung mesenchyme and epithelium is an important upstream regulator of *Wnt2* expression in the mesenchyme (Yin et al., 2008), however, our data show that *Fgf9* expression levels are unchanged in *Hox5* triple mutants. Future work will determine whether *Fgf9* signaling acts upstream or in a parallel to *Hox5* genes to control *Wnt2/2b* expression in the lung mesenchyme.

Wnt/β-catenin signaling is a critical upstream regulator of *Bmp4* expression in the distal lung epithelium and this regulatory relationship is essential for proper PD patterning of the airway epithelium (Shu et al., 2005). Loss of *Bmp4* signaling leads to similar defects in proximal distal patterning and has been reported to be critical for inhibiting the expansion of Sox2+ proximal lung progenitors and promoting Sox9+ distal progenitor development in the distal airway (Domyan et al., 2011). Consistent with these reports, loss of canonical Wnt/β-catenin signaling in the distal epithelium observed in *Hox5* triple mutants results in the down-regulation of *Bmp4* expression in the distal epithelium and leads, in turn, to the distal expansion of Sox2. These data, together with previous work, identify a *Hox5-Wnt2/2b-Bmp4* signaling axis that is required for the proper growth and PD patterning of the lung during embryogenesis.

Finally, we show that the addition of Wnt2/2b ligand into the lung explant culture media is sufficient to rescue the downstream defects observed in *Hox5* triple mutants. *Hox5* triple mutant lungs cultured in Wnt2/2b-enriched media reach nearly the same total number of distal branch tips as control lung explants and, perhaps more remarkably, also exhibit normalized Sox2/Sox9 PD patterning and restored *Bmp4* and SMA expression comparable to controls. These data provide strong evidence that the primary cause of the lung defects of *Hox5* triple mutants is the reduction of *Wnt2/2b* expression in the mesenchyme and demonstrate that redundant *Hox5* function is responsible for maintaining regional mesenchymal *Wnt* signaling in the developing lung.

Experimental Procedures

Mice and histology

Generation of the *Hoxa5* mutant mouse used in this study is outlined in Figure S4. A detailed description of the generation of this mouse is described in the Supplemental Experimental Methods. The Axin2-LacZ reporter mouse used in this study has been

previously described (Lustig et al., 2002). Control mice included both wildtype embryos and low-allele littermates from *Hox5* and *Hox5/Axin2*$^{LacZ/+}$ crosses. The results were identical, and thus we use the term "control" throughout for clarity. E18.5 lungs were dissected in PBS, fixed in formalin overnight, and dehydrated through graded alcohols and stored in 70% ethanol at 4°C. Lungs were then vacuum-embedded in paraffin, sectioned at 5μm and stained with hematoxylin and eosin. All experiments were performed following protocols approved by the University of Michigan's Institutional Committee on the Use and Care of Animals.

In situ hybridization and Immunohistochemistry

For section *in situ* hybridization (ISH) and immunohistochemistry (IHC), embryos were collected in PBS and fixed overnight in 4% paraformaldehyde in PBS at 4 °C. Embryos were then rinsed in PBS and immersed in 30% sucrose at 4°C overnight before embedding into optimal cutting temperature (OCT) media. Frozen sections 12–16 μm in size were cut, and slides were stored at −80 °C. Details of the section ISH procedure and a complete list of ISH probes and antibodies used for IHC in this report are provided in the Supplemental Experimental Methods. LacZ histochemical staining of embryos was performed as previously described (Spence et al., 2009).

Lung explant cultures

Lung explant cultures were performed *in vitro*, as previously described (Del Moral and Warburton, 2010). E12.5 lungs were cultured on Nucleopore polycarbonate track-etch membranes for up to 96 h at 37 °C in a 5% CO_2 incubator. Images of explants were taken on a Leica MZ125 stereomicroscope. Constructs and methods used to generate Wnt2/2b-enriched media for lung explant cultures have been previously described (Najdi et al., 2012). Identical results were obtained using either Wnt2 or Wnt2b enriched media (n=3 of each).

RNA isolation and quantitative RT-PCR

RNA was isolated from mouse lungs with the Qiagen RNeasy Micro Kit. Quantitative RT-PCR (qRT-PCR) was carried out using Roche FastStart SYBR Green Master Mix and the Applied Biosystems StepOnePlus Real-time PCR system (Life Technologies). Primer sequences used are provided in Table S1. Relative expression values were calculated as $2^{-\Delta\Delta Ct}$ and values of controls were normalized to 1. GAPDH served as an internal control for normalization in all qRT-PCR experiments. All data are shown as the mean of at least three independent biological replicates; error bars represent SEM. Statistical differences between experimental and control groups were assessed with Prism software, using multiple *t* tests. Results were considered statistically significant at $P < 0.05$. All experiments were repeated at least three times in independent experiments.

Supplementary Material

Refer to Web version on PubMed Central for supplementary material.

Acknowledgments

We acknowledge E. Hughes, K. Childs, G. Gavrilina and D. VanHeyningen for the preparation of gene-targeted mice and the Transgenic Animal Model Core of the University of Michigan's Biomedical Research Core Facilities. Core support was provided by the University of Michigan Cancer Center, NIH grant number CA46592 and the University of Michigan George M. O'Brien Renal Core Center, NIH grant number P30DK08194. We thank E. Morrisey, X. Sun, B. Hogan, and D. Martin for kindly providing ISH probes used in this study and Holly R. Fischer for generating the graphical abstract. This work was supported by a Ruth L. Kirschstein National Research Service Award (NSRA) training Grant 5 T32 HL 7749-20 and a National Center for Research Resources grant number UL1RR024986 to SMH. This research was also supported by the National Heart, Lung, and Blood Institute (NHLBI) R01-HL119215 to J.R.S. and D.M.W.

References

Aubin J, Lemieux M, Tremblay M, Berard J, Jeannotte L. Early postnatal lethality in Hoxa-5 mutant mice is attributable to respiratory tract defects. Dev Biol. 1997; 192:432–445. [PubMed: 9441679]

Bellusci S, Furuta Y, Rush MG, Henderson R, Winnier G, Hogan BL. Involvement of Sonic hedgehog (Shh) in mouse embryonic lung growth and morphogenesis. Development. 1997; 124:53–63. [PubMed: 9006067]

Boucherat O, Montaron S, Berube-Simard FA, Aubin J, Philippidou P, Wellik DM, Dasen JS, Jeannotte L. Partial functional redundancy between Hoxa5 and Hoxb5 paralog genes during lung morphogenesis. Am J Physiol Lung Cell Mol Physiol. 2013; 304:L817–830. [PubMed: 23585229]

Chang DR, Martinez Alanis D, Miller RK, Ji H, Akiyama H, McCrea PD, Chen J. Lung epithelial branching program antagonizes alveolar differentiation. Proc Natl Acad Sci U S A. 2013; 110:18042–18051. [PubMed: 24058167]

Cohen ED, Ihida-Stansbury K, Lu MM, Panettieri RA, Jones PL, Morrisey EE. Wnt signaling regulates smooth muscle precursor development in the mouse lung via a tenascin C/PDGFR pathway. J Clin Invest. 2009; 119:2538–2549. [PubMed: 19690384]

Del Moral PM, Warburton D. Explant culture of mouse embryonic whole lung, isolated epithelium, or mesenchyme under chemically defined conditions as a system to evaluate the molecular mechanism of branching morphogenesis and cellular differentiation. Methods Mol Biol. 2010; 633:71–79. [PubMed: 20204620]

Di Meglio T, Kratochwil CF, Vilain N, Loche A, Vitobello A, Yonehara K, Hrycaj SM, Roska B, Peters AH, Eichmann A, et al. Ezh2 orchestrates topographic migration and connectivity of mouse precerebellar neurons. Science. 2013; 339:204–207. [PubMed: 23307742]

Domyan ET, Ferretti E, Throckmorton K, Mishina Y, Nicolis SK, Sun X. Signaling through BMP receptors promotes respiratory identity in the foregut via repression of Sox2. Development. 2011; 138:971–981. [PubMed: 21303850]

Herriges M, Morrisey EE. Lung development: orchestrating the generation and regeneration of a complex organ. Development. 2014; 141:502–513. [PubMed: 24449833]

Kessel M, Gruss P. Murine developmental control genes. Science. 1990; 249:374–379. [PubMed: 1974085]

Kimura S, Hara Y, Pineau T, Fernandez-Salguero P, Fox CH, Ward JM, Gonzalez FJ. The T/ebp null mouse: thyroid-specific enhancer-binding protein is essential for the organogenesis of the thyroid, lung, ventral forebrain, and pituitary. Genes Dev. 1996; 10:60–69. [PubMed: 8557195]

Lustig B, Jerchow B, Sachs M, Weiler S, Pietsch T, Karsten U, van de Wetering M, Clevers H, Schlag PM, Birchmeier W, et al. Negative feedback loop of Wnt signaling through upregulation of conductin/axin2 in colorectal and liver tumors. Mol Cell Biol. 2002; 22:1184–1193. [PubMed: 11809809]

Mallo M, Wellik DM, Deschamps J. Hox genes and regional patterning of the vertebrate body plan. Developmental Biology. 2010; 344:7–15. [PubMed: 20435029]

Manley NR, Capecchi MR. Hox group 3 paralogs regulate the development and migration of the thymus, thyroid, and parathyroid glands. Dev Biol. 1998; 195:1–15. [PubMed: 9520319]

Miller MF, Cohen ED, Baggs JE, Lu MM, Hogenesch JB, Morrisey EE. Wnt ligands signal in a cooperative manner to promote foregut organogenesis. Proc Natl Acad Sci U S A. 2012; 109:15348–15353. [PubMed: 22949635]

Mollard R, Ghyselinck NB, Wendling O, Chambon P, Mark M. Stage-dependent responses of the developing lung to retinoic acid signaling. Int J Dev Biol. 2000; 44:457–462. [PubMed: 11032179]

Morrisey EE, Hogan BLM. Preparing for the First Breath: Genetic and Cellular Mechanisms in Lung Development. Developmental Cell. 2010; 18:8–23. [PubMed: 20152174]

Mucenski ML, Wert SE, Nation JM, Loudy DE, Huelsken J, Birchmeier W, Morrisey EE, Whitsett JA. beta-Catenin is required for specification of proximal/distal cell fate during lung morphogenesis. J Biol Chem. 2003; 278:40231–40238. [PubMed: 12885771]

Najdi R, Proffitt K, Sprowl S, Kaur S, Yu J, Covey TM, Virshup DM, Waterman ML. A uniform human Wnt expression library reveals a shared secretory pathway and unique signaling activities. Differentiation. 2012; 84:203–213. [PubMed: 22784633]

Rockich BE, Hrycaj SM, Shih HP, Nagy MS, Ferguson MA, Kopp JL, Sander M, Wellik DM, Spence JR. Sox9 plays multiple roles in the lung epithelium during branching morphogenesis. Proc Natl Acad Sci U S A. 2013; 110:E4456–4464. [PubMed: 24191021]

Rousso DL, Gaber ZB, Wellik D, Morrisey EE, Novitch BG. Coordinated actions of the forkhead protein Foxp1 and Hox proteins in the columnar organization of spinal motor neurons. Neuron. 2008; 59:226–240. [PubMed: 18667151]

Sekine K, Ohuchi H, Fujiwara M, Yamasaki M, Yoshizawa T, Sato T, Yagishita N, Matsui D, Koga Y, Itoh N, et al. Fgf10 is essential for limb and lung formation. Nat Genet. 1999; 21:138–141. [PubMed: 9916808]

Shu W, Guttentag S, Wang Z, Andl T, Ballard P, Lu MM, Piccolo S, Birchmeier W, Whitsett JA, Millar SE, et al. Wnt/β-catenin signaling acts upstream of N-myc, BMP4, and FGF signaling to regulate proximal–distal patterning in the lung. Developmental Biology. 2005; 283:226–239. [PubMed: 15907834]

Spence JR, Lange AW, Lin SC, Kaestner KH, Lowy AM, Kim I, Whitsett JA, Wells JM. Sox17 regulates organ lineage segregation of ventral foregut progenitor cells. Dev Cell. 2009; 17:62–74. [PubMed: 19619492]

Tompkins DH, Besnard V, Lange AW, Keiser AR, Wert SE, Bruno MD, Whitsett JA. Sox2 activates cell proliferation and differentiation in the respiratory epithelium. Am J Respir Cell Mol Biol. 2011; 45:101–110. [PubMed: 20855650]

Weaver M, Yingling JM, Dunn NR, Bellusci S, Hogan BL. Bmp signaling regulates proximal-distal differentiation of endoderm in mouse lung development. Development. 1999; 126:4005–4015. [PubMed: 10457010]

Wellik DM, Hawkes PJ, Capecchi MR. Hox11 paralogous genes are essential for metanephric kidney induction. Genes Dev. 2002; 16:1423–1432. [PubMed: 12050119]

Xu B, Hrycaj SM, McIntyre DC, Baker NC, Takeuchi JK, Jeannotte L, Gaber ZB, Novitch BG, Wellik DM. Hox5 interacts with Plzf to restrict Shh expression in the developing forelimb. Proc Natl Acad Sci U S A. 2013; 110:19438–19443. [PubMed: 24218595]

Yallowitz AR, Hrycaj SM, Short KM, Smyth IM, Wellik DM. Hox10 genes function in kidney development in the differentiation and integration of the cortical stroma. PLoS One. 2011; 6:e23410. [PubMed: 21858105]

Yin Y, White AC, Huh SH, Hilton MJ, Kanazawa H, Long F, Ornitz DM. An FGF–WNT gene regulatory network controls lung mesenchyme development. Developmental Biology. 2008; 319:426–436. [PubMed: 18533146]

Highlights

1. All three *Hox5* paralogous genes play redundant roles in the developing lung.
2. *Hox5* triple mutants exhibit severely hypoplastic lungs with altered proximal-distal patterning.
3. Loss of *Hox5* function leads to loss of mesenchymal *Wnt2/2b* expression.
4. The addition of Wnt2/2b ligand rescues *Hox5* phenotypes, demonstrating sufficiency.

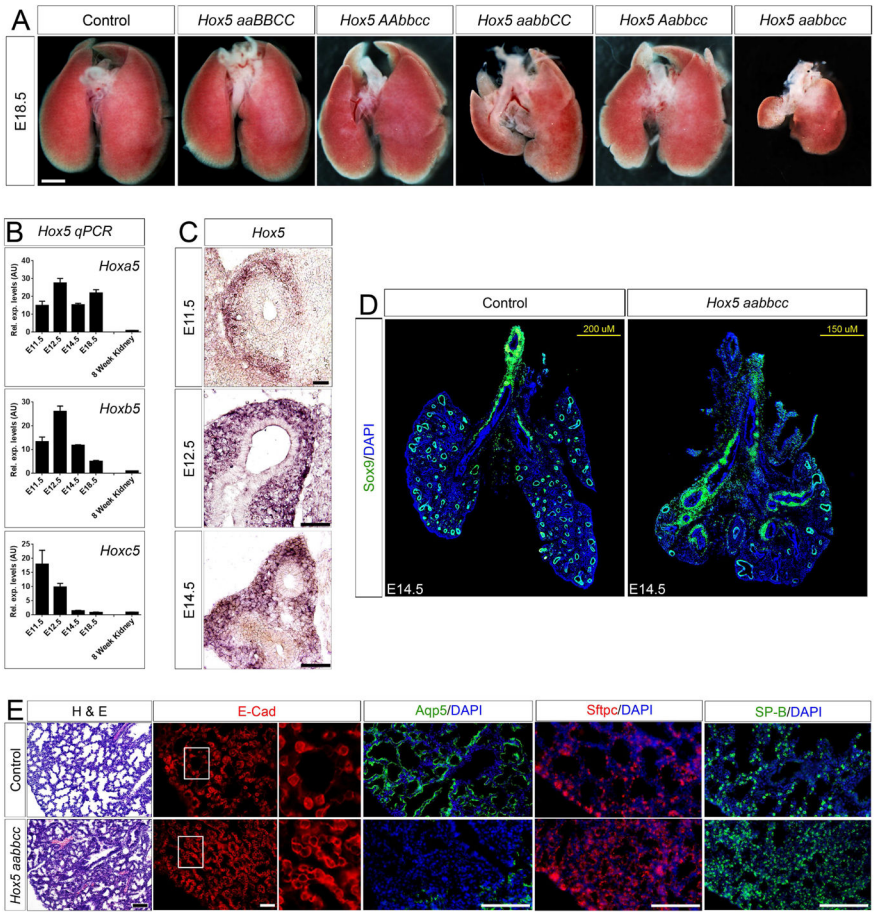

Figure 1. *Hox5* expression and triple mutant phenotypes during embryogenesis

(A) E18.5 lungs from the *Hox5* mutant allelic series. Lung morphology shows minor defects in *Hoxa5* single mutants compared to controls, single mutants of *Hoxb5* or *Hoxc5* or double *Hoxb5/Hoxc5* mutants are indistinguishable from controls. *Hoxa5/Hoxb5* double mutants and five-allele mutants (*Hox5 Aabbcc* shown here) show phenotypes, but the severity of the phenotype is drastically exacerbated with loss-of-function of all three *Hox5* paralogs (*Hox5 aabbcc*). Scale bar represents 1mm in all panels.

(B) qPCR analysis for each of the three *Hox5* paralogs through embryonic stages shows high expression of all three paralogs, *Hoxa5*, *Hoxb5* and *Hoxc5* at early time points. *Hoxa5* expression remains high throughout embryonic development, while both *Hoxb5* and *Hoxc5* decrease from E14.5.

(C) *In situ* hybridization analyses using combined probes for *Hoxa5*, *Hoxb5* and *Hoxc5* show that all three paralogs are expressed only in the mesenchyme and not the endoderm of the developing lung. Scale bars represent 50uM.

(D) Proximodistal patterning is disrupted in *Hox5* triple mutant animals. Control E14.5 lungs show normal expression of Sox9 in the proximal mesenchyme and distal epithelium. In *Hox5* triple mutant animals, Sox9 mesenchymal expression is expanded into very distal regions of the lung.

(E) Characterization of distal lung defects in E18.5 *Hox5* triple mutants. H&E staining of histological sections shows less saccule formation and thickening of the lung perenchyma in

Hox5 triple mutants compared to controls. Immunostaining for E-cadherin shows an increase in cuboidal epithelium in *Hox5* mutants compared to controls and cell type specific markers reveal large stretches of the *Hox5* distal lung that are completely devoid of AECI cells as visualized by Aqp5 and large increases in the AECII cells (Sftpc and SP-B). Scale bars represent 100uM in all panels.

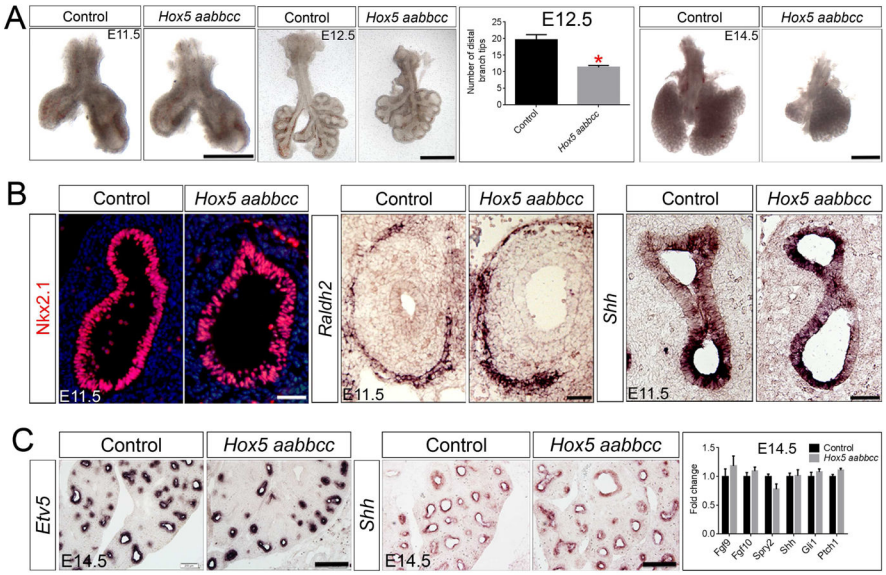

Figure 2. Lung initiation events are unaffected in *Hox5 aabbcc* triple mutants

(A) *Hox5* mutant lungs are indistinguishable from controls at E11.5, but become increasingly hypoplastic relative to controls from E12.5. Scale bars represent 0.5mm in all panels.

(B) Markers of lung initiation are not disrupted in *Hox5* triple mutant embryos. Immunostaining for Nkx2.1 and ISH analyses for *Raldh2* and *Shh* show no differences in expression between controls and mutants. Scale bars represent 50uM in all panels.

(C) Fgf and Shh signaling pathways show no disruption in *Hox5* mutant lungs. ISH analyses of *Etv5*, a downstream read-out of Fgf signaling and *Shh* show no perturbations in levels or patterns in *Hox5* mutants compared to controls. Scale bars represent 200uM. qPCR analyses show no changes in levels of any Fgf or Hh pathway component measured, including *Fgf9, Fgf10, Spry2, Shh, Gli1* or *Ptch1*.

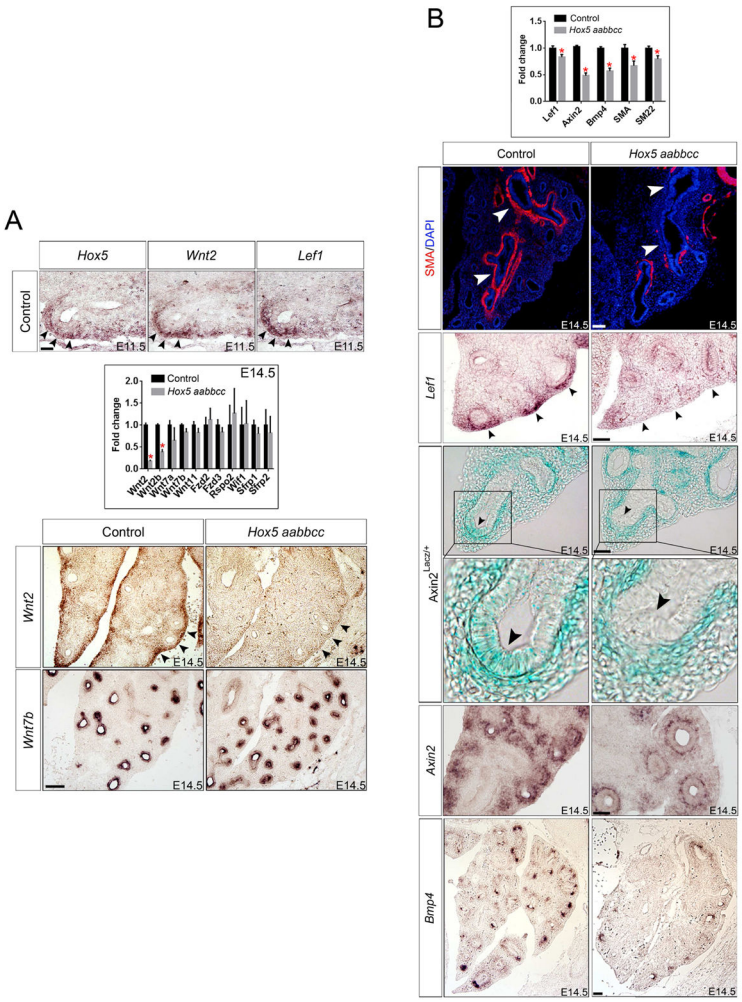

Figure 3. *Hox5* genes regulate canonical Wnt/β-catenin signaling

(A) *Hox5* expression overlaps with mesenchymal *Wnt* signaling in the developing lung and both mesenchymal *Wnt* ligands are down-regulated in *Hox5* mutants. ISH analyses with combined *Hox5* probes, *Wnt2* and *Lef1* on adjacent sections show a complete overlap in expression patterns for these genes, consistent with a regulatory relationship. Scale bar represents 50uM in all panels. qPCR analyses shows significant reduction of the two mesenchymal *Wnt* factors in the lung, *Wnt2* and *Wnt2b*. Epithelial *Wnt* ligands, *Wnt7a* and *Wnt7b* and other *Wnt* inhibitors and receptors are not affected in *Hox5* mutants compared to controls. These results are confirmed by ISH, showing that *Wnt2* is markedly down-regulation in the mesenchyme of *Hox5* mutants compared to controls while *Wnt7b* expression appears unaffected. Scale bar represents 200uM in all panels.

(B) Genes downstream of the *Wnt* pathway in the developing lung are reduced in *Hox5* mutants. qPCR analyses shows a reduction in *Lef1, Axin2, Bmp4, SMA* and *SM22*. These analyses are confirmed by immunostaining with SMA, ISH of both *Lef1* and *Bmp4*. Using both ISH and an Axin2-LacZ reporter allele crossed into *Hox5* mutants, epithelial staining is specifically absent in the epithelium of *Hox5* mutants (arrowheads) although mesenchymal staining appears unaffected. Scale bars represent 50uM in all panels.

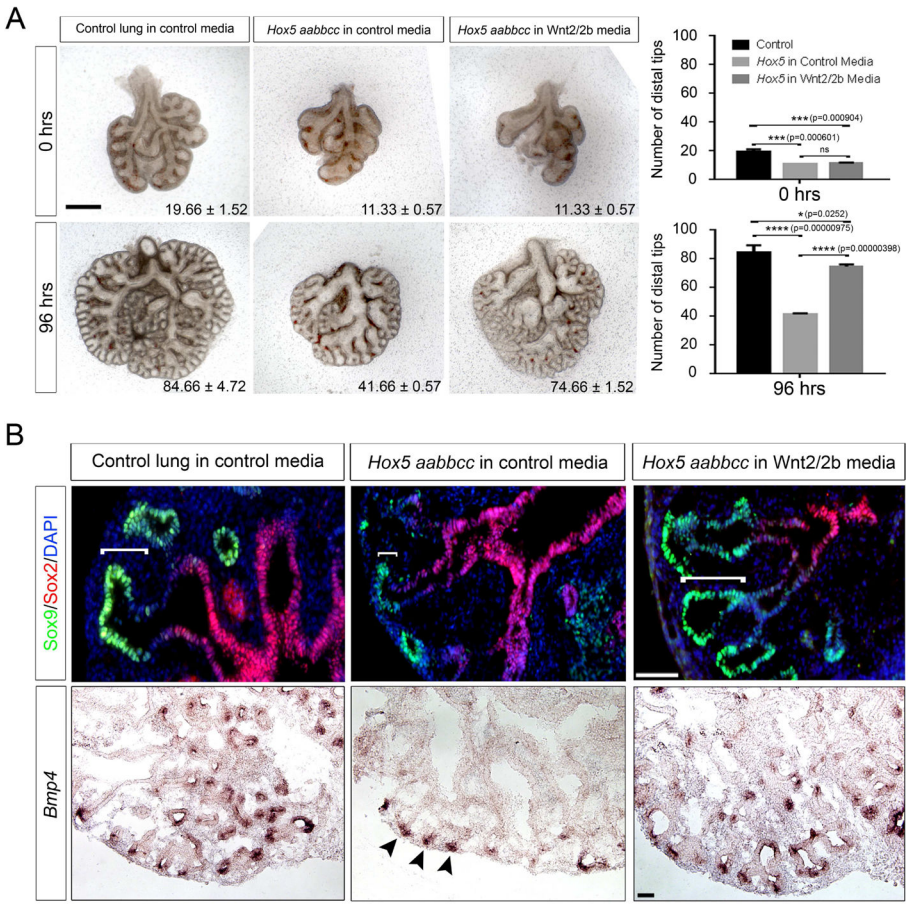

Figure 4. Treatment of *Hox5 aabbcc* mutant lung explants with Wnt2/2b ligand rescues branching and restores proper PD patterning

(A) Treatment of *Hox5* mutant lungs with *Wnt2/2b* ligand rescues branching phenotype. *Hox5* mutant embryonic and control lungs were dissected at E12.5 and treated for 96 hours with or without Wnt2/2b enriched, serum-free media. Control lungs increased their branch tips from an average of 19.66 to 84.66 over this time period. Despite defects already apparent at this stage in *Hox5* mutant lungs (11.33 tips), treatment with *Wnt2/2b* for 96 hours increased the total branch tip number from 41.66 to 74.66, nearly reaching control branch tip numbers. Scale bar represents 0.5mm in all panels.

(B) *Wnt2/2b* rescue restores normal PD patterning to *Hox5* triple mutants. Sectioning lung tissue from these experiments at the end of culture and staining with PD markers Sox2 and Sox9 shows that control lungs develop the same normal pattern observed *in vivo* with proximal Sox2 and distal Sox9 expression. Sox2 expression is extended distally in *Hox5* mutants with a severe reduction in Sox9 distal staining as observed *in vivo*. Treatment of *Hox5* mutant lungs with *Wnt2/2b* restores normal patterning as visualized by these two markers. Scale bar represents 50uM in all panels. *Bmp4* distal tip expression also appears identical to what is observed *in vivo* in control lung cultures, and *Hox5* mutants show the same severe reduction in this expression. Treatment with *Wnt2/2b* enriched media restores this expression after 96 hours in culture. Scale bar represents 50uM in all panels.